ECMWF COPERNICUS REPORT

Copernicus Climate Change Service

Product Quality Assessment Report (PQAR) – ANNEX A for products CO2_GOS_OCFP, CH4_GOS_OCFP (v7.3, 2009-mid2020) & CH4_GOS_OCPR (v9.0, 2009-mid2020)

C3S_312b_Lot2_DLR – Atmosphere

Issued by: Hartmut Boesch, Jasdeep Anand, and Antonio Di Noia, University of Leicester, Leicester, UK

Date: 18/02/2021

Ref: C3S_D312b_Lot2.2.3.2-v3.0_PQAR-GHG_ANNEX-A_v5.0

Official reference number service contract: 2018/C3S_312b_Lot2_DLR/SC1

IMPLEMENTED BY ECMWF

Contributors

INSTITUTE OF ENVIRONMENTAL PHYSICS (IUP), UNIVERSITY OF BREMEN, BREMEN, GERMANY (IUP)
M. Buchwitz

UNIVERSITY OF LEICESTER, LEICESTER, UK (UoL)
H. Boesch
J. Anand
P. Somkuti
R. Parker
A. Di Noia

Table of Contents

History of modifications

Version	Date	Description of modification	Chapters / Sections
1.1	20-October-2017	New document for data set CDR1 (2009-2016)	All
2.0	4-October-2018	Update for CDR2 (2009-2017) Updated statistics and plots for v7.2 data	All
3.0	12-August-2019	Update for CDR3 (2009-2018)	All
3.1	03-November-2019	Update after review by Assimila: Primarily correction of typos. Some additional information added.	All
4.0	18-August-2020	Update for CDR4 (2009-2019)	All
5.0	18-February-2020	Update for CDR5 (2009-mid2020)	All

Related documents

Reference ID	Document
D1	Main PQAR: Buchwitz, M., et al., Product Quality Assessment Report (PQAR) – Main document for Greenhouse Gas (GHG: CO_2 & CH_4) data set CDR 5 (01.2003-06.2020), project C3S_312b_Lot2_DLR – Atmosphere, v5.0, 2021. ***Important Note:*** *This document is an ANNEX to the Main PQAR document and contains the quality assessment results of the data provider.* ***For the final overall quality assessment results of the data products described in this document see the Main PQAR document.***
D2	Boesch, H., Anand, J., and Di Noia, A.: Algorithm Theoretical Basis Document (ATBD) – ANNEX A for products CO2_GOS_OCFP and CH4_GOS_OCFP (v7.3, 2009-mid2020) & CH4_GOS_OCPR (v9.0, 2009-mid2020), project C3S_312b_Lot2_DLR – Atmosphere, v5.0, 2021.

Acronyms

Acronym	Definition
C3S	Copernicus Climate Change Service
CDS	(Copernicus) Climate Data Store
ECMWF	European Centre for Medium Range Weather Forecasting
ECV	Essential Climate Variable
ESA	European Space Agency
EU	European Union
GHG	GreenHouse Gas
GMES	Global Monitoring for Environment and Security
GOSAT	Greenhouse Gases Observing Satellite
IUP	Institute of Environmental Physics (IUP) of the University of Bremen, Germany
KPI	Key Performance Indicator
L1	Level 1
L2	Level 2
L3	Level 3
L4	Level 4
LMD	Laboratoire de Météorologie Dynamique
MACC	Monitoring Atmospheric Composition and Climate, EU GMES project
NOAA	National Oceanic and Atmospheric Administration
OCO	Orbiting Carbon Observatory
PCA	Principal Component Analysis
ppb	Parts per billion
ppm	Parts per million
QA	Quality Assurance
QC	Quality Control
SCIAMACHY	SCanning Imaging Absorption spectroMeter for Atmospheric ChartographY
SWIR	Short Wave Infra Red
TCCON	Total Carbon Column Observing Network
TIR	Thermal Infra Red
TR	Target Requirements
TRD	Target Requirements Document
UoL	University of Leicester, United Kingdom

General definitions

Table 1 lists some general definitions relevant for this document.

Table 1: General definitions.

Item	Definition
XCO_2	Column-averaged dry-air mixing ratios (mole fractions) of CO_2
XCH_4	Column-averaged dry-air mixing ratios (mole fractions) of CH_4
L1	Level 1 satellite data product: geolocated radiance (spectra)
L2	Level 2 satellite-derived data product: Here: CO_2 and CH_4 information for each ground-pixel
L3	Level 3 satellite-derived data product: Here: Gridded CO_2 and CH_4 information, e.g., 5 deg times 5 deg, monthly
L4	Level 4 satellite-derived data product: Here: Surface fluxes (emission and/or uptake) of CO_2 and CH_4

Scope of document

This document is a Product Quality Assessment Report (PQAR) for the Copernicus Climate Change Service (C3S, https://climate.copernicus.eu/) greenhouse gas (GHG) component as covered by project C3S_312b_Lot2.

Within this project satellite-derived atmospheric carbon dioxide (CO_2) and methane (CH_4) Essential Climate Variable (ECV) data products will be generated and delivered to ECMWF for inclusion into the Copernicus Climate Data Store (CDS) from which users can access these data products and the corresponding documentation.

The GHG satellite-derived data products are:

- Column-averaged dry-air mixing ratios (mole fractions) of CO_2 and CH_4, denoted XCO_2 (in parts per million, ppm) and XCH_4 (in parts per billion, ppb), respectively.
- Mid/upper tropospheric mixing ratios of CO_2 (in ppm) and CH_4 (in ppb).

This document describes the validation / quality assessment of the C3S products CO2_GOS_OCFP (v7.3), CH4_GOS_OCFP (v7.3) and CH4_GOS_OCPR (v9.0).

These products are XCO_2 and XCH_4 Level 2 products as retrieved from GOSAT using algorithms developed at the University of Leicester, UK.

Executive summary

XCO_2 and XCH_4 retrieved from the Greenhouse Gases Observing Satellite (GOSAT) have been derived using retrieval algorithms developed by the University of Leicester (UoL) for C3S. In this document we compare the GOSAT observations against highly accurate and verified ground-based measurements from the Total Carbon Column Observation Network (TCCON), in order to determine their accuracy and stability against the criteria set in the Target Requirements Document (TRD, *TRD GHG, 2017; TRD GAD GHG, 2020*)

The following products were verified against the TCCON GGG2014 dataset:

- CO2_GOS_OCFP (v 7.3)
- CH4_GOS_OCFP (v 7.3)
- CH4_GOS_OCPR (v 9.0)

GOSAT observations were spatially and temporally co-located with TCCON sites based on a fixed 555 km radius and ±2 hours temporal window. For CO2_GOS_OCFP additional co-location was performed using a technique similar to *Wunch et al., 2011*, in which the mid-tropospheric temperature is used as a proxy for CO_2 gradients. A number of statistics (e.g. relative accuracy, stability) based on the GOSAT-TCCON agreement were calculated for each product, which are detailed in the Main PQAR document. The probability that each product met the Target Requirement (TR) for accuracy and stability was also calculated. Qualitative analysis was also performed by comparing the seasonal average of each dataset against the CarbonTracker XCO_2 and XCH_4 Monitoring Atmospheric Composition and Climate (MACC) model.

Overall, the UoL products are found to be highly stable, with a >90% probability of meeting the stability (linear drift) TR. The single measurement precision (1-sigma) reported by each product was also found to meet at least baseline requirement determined in the TRD.

1. Product validation methodology

1.1 The UoL CO_2 and CH_4 products

The UoL CO_2 and CH_4 ECV products are retrieved from calibrated GOSAT SWIR spectra using the OCO (Orbiting Carbon Observatory) full-physics retrieval algorithm discussed in *Boesch et al., 2011*. The retrieval algorithm obtains the column-averaged dry air mass mixing ratios of these gases (XCO_2 and XCH_4, respectively) from a simultaneous fit of the near-infrared O_2-A band spectrum at 0.76 µm and the CO_2 bands at 1.61 and 2.06 µm as measured by the GOSAT instrument.

The retrieval algorithm employs an iterative retrieval scheme based on Bayesian optimal estimation to estimate a set of atmospheric, surface and instrument parameters from measured spectral radiances. The forward model consists of coupled radiative transfer (RT) and solar spectrum models, calculating the monochromatic spectrum of light originating from the Sun, passing through the atmosphere, reflecting from Earth's surface or scattering back from the atmosphere, exiting at the top of the atmosphere (TOA) and entering the instrument. TOA radiances are then passed to the instrument model to simulate measured radiances at the appropriate spectral resolution. The forward model employs the LIDORT RT model combined with a fast 2-orders-of-scattering vector radiative transfer code discussed in *Natraj et al., 2008*. Additionally, the code has two options to accelerate the RT component of the retrieval algorithm: the low stream interpolation (LSI) method described in *O'Dell*, 2010, and the principal component analysis (PCA)-based fast RT scheme described in *Somkuti et al.,* 2017.

The OCFP algorithm retrieves a CO_2 or CH_4 profile together with a number of additional parameters including scaling factors for H_2O and temperature profile, surface pressure, surface albedo, solar induced fluorescence (SIF) and spectral slope per band, spectral shift and stretch/squeeze, extinction profiles of two aerosol profiles and one cirrus cloud profile. XCO_2 or XCH_4, error metrics and averaging kernels are calculated from the retrieved CO_2 or CH_4 profile following algorithm convergence. Fast cloud screening based on clear-sky surface pressure retrieved from the O_2 A band is applied in pre-processing to reduce processing overhead on unrequired contaminated soundings, whilst a number of post-processing quality filters are applied for removal of low quality retrievals.

The OCPR algorithm also retrieves XCH_4 by using the CO_2 proxy method defined in *Frankenberg et al., 2011*. Making use of lower atmospheric CO_2 variation as compared to CH_4, coupled with the spectral proximity of CO_2 and CH_4 absorption bands, this allows CO_2 to be used as a light path proxy, minimising spectral artefacts due to aerosol scattering and instrumental effects, as discussed in, *Butz et al., 2010*. CH_4 and CO_2 retrievals are carried out sequentially with channels at 1.65 µm and 1.61 µm respectively. To calculate the true XCH_4 value, the XCH_4:XCO_2 ratio is multiplied by a model XCO_2 concentration. The modelled XCO_2 is taken from the median of a CO_2 model ensemble comprising data from GEOS-Chem (University of Edinburgh), NOAA CarbonTracker, *Peters et al., 2007*, and LMDZ / MACC-II *Chevallier et al., 2010*, convolved with scene-dependent instrument averaging kernels obtained from the GOSAT CO_2 retrieval. Fast cloud screening based on clear-sky

surface pressure retrieved from the O_2 A band is applied in pre-processing to reduce processing overhead on unrequired contaminated soundings, whilst a number of post-processing quality filters are applied for removal of low quality retrievals.

1.2 TCCON

The Total Carbon Column Observing Network (TCCON) is a global network of Fourier transform spectrometers built for the purpose of validating space-borne measurements of XCO_2 and XCH_4, *Wunch et al., 2010*. TCCON observes these gases with a precision on mole fractions of ~0.15% and ~0.2% for CO_2 and CH_4 respectively, *Toon et al., 2009*. Although providing highly accurate measurements, the sparseness of the TCCON sites presents a challenge for validation, offering precise GHG measurements for only a limited range of geographic and meteorological conditions.

Additional considerations should be made when validating with TCCON data for differing sensitivity of instruments between TCCON and the satellite instrument, reflected in a priori information used for each retrieval. Removing the influence of the retrieval a priori and replacing with the TCCON a priori allows for a fairer comparison between the two datasets, although slight differences in retrieval methodologies prevent a 1:1 comparison. Users of C3S data (particularly in the modelling community) should note that the published C3S products are not corrected with TCCON a priori information (due to a priori differences between sites), and so will find slightly worse correlations between satellite retrieved GHGs and TCCON values in their own comparisons. TCCON data used for error assessments come from the GGG2014 collection (available from https://tccondata.org.

The TCCON stations chosen to validate the UoL datasets are summarised in Table 2. These stations were chosen for their long data record in order to characterise the local seasonal cycle of CO_2 and CH_4. Remote stations such as Ascension Island were thought to be too distant from land to validate nadir (land) measurements, and so were also excluded from this analysis.

Table 2: The TCCON stations used to validate the UoL GOSAT data products.

Station name	Latitude (°)	Longitude (°)
Sodankyla	67.37	26.63
Bialystok	53.23	23.03
Bremen	53.10	8.85
Karlsruhe	49.10	8.44
Orleans	47.97	2.11
Garmisch	47.48	11.06
Park Falls	45.95	-90.27
Lamont	36.60	-97.49
Tsukuba	36.05	140.12
Saga	33.24	130.29
Darwin	-12.42	130.89
Wollongong	-34.41	150.88
Lauder	-45.04	169.68

1.3 Co-location between TCCON and UoL GOSAT data

The TCCON instruments produce calibrated measurements of XCO_2 and XCH_4, and are an ideal validation dataset to compare against GOSAT data. GOSAT data must first be spatially and temporally matched against co-incident TCCON measurements; the process of matching these two datasets is referred to as "co-location" in this work. Below we detail the UoL co-location techniques, whose methodology has a bearing on subsequent error statistics.

1.3.1 Co-location using radial distance from TCCON site ("Radial" method)

This method is used in the CH4_GOS_OCFP and CH4_GOS_OCPR datasets to identify GOSAT-TCCON pairs to use in the post-retrieval filtering and bias correction calculation. We also use this method to perform all the validation detailed in this work for these datasets.

1.3.1.1 Spatial

GOSAT points are co-located with TCCON sites based on their distance to station, regardless of geographic location. This is carried out with the delineation of a buffer around each TCCON site (555 km radius in the work presented here, equivalent to ~5˚ at the equator) using the Haversine formula to calculate the great-circle distance between TCCON site location and central coordinates of each satellite observation. This distance-based method has a further advantage of eliminating satellite point selection for those lying beyond the defined radius, whilst the previous grid-box based method would include points beyond this up to those approximately within the hypotenuse for a grid box quartile.

1.3.1.2 Temporal

Matching GOSAT soundings with TCCON sites for time is a comparatively simple operation, selecting only those TCCON values whose observation time falls within ±2 hours of each GOSAT sounding time. The average is taken of all TCCON points fitting these criteria for each GOSAT sounding to provide the TCCON value against which to compare.

1.3.2 Co-location using free-troposphere potential temperature ("T700" method)

This method is used exclusively for the filtering and bias correction of the CO2_GOS_OCFP dataset, and is used in this work to give alternative validation statistics which are consistent with how the bias correction was derived.

XCO_2 has been observed to correlate with free-troposphere potential temperature, and so this quantity can be used to identify air masses that are coincident over TCCON sites more precisely than does a simple geographic constraint. This technique has previously been used to calibrate and validate GOSAT XCO_2 observations by *Wunch et al., 2011*. For this work we use the mid-tropospheric temperature at 700 hPa taken from ECMWF (see *D2*) as a proxy for CO_2 gradients, which allows for a greater number of GOSAT observations to be compared with TCCON. Co-incident GOSAT observations are determined using the following criteria:

1.3.2.1 Spatial and temperature

First, GOSAT observations that fall within 10° latitude and 30° longitude of a given TCCON site are identified and considered for co-location. The temperature at 700 hPa is taken from the TCCON a priori information provided in the GGG2014 dataset, while the corresponding temperature for each GOSAT observation is estimated from the temperature profile used in the GOSAT retrieval state vector. A GOSAT observation is co-located with a TCCON site if the temperature is within ±2 K of that estimated over the TCCON site.

For Japanese TCCON sites we use a 10° longitude range to identify possible observations, in order to decrease the influence of observations that have been contaminated by high XCO_2 from Chinese emissions, which would otherwise bias comparisons.

1.3.2.2 Temporal

For a given GOSAT observation, all TCCON observations that meet the ±2 K criterion and were made within ±10 days of the GOSAT observation are averaged together to give a single TCCON value to compare against the GOSAT XCO_2.

2. Validation Results

To assess the quality of each product, the matched GOSAT-TCCON datasets are directly compared through linear regression. Statistics are collated over each individual TCCON site, as well as all of them combined. While both land and glint observations are considered for this exercise, only land observations will be used to produce a final assessment of the products, as the main application of these datasets will be to improve our knowledge of terrestrial carbon sources and sinks.

The most significant metrics calculated in this validation exercise are:

- **Single ground pixel random error** (or "single measurement precision", 1-sigma): Computed as the standard deviation of the difference of the single satellite measurement with TCCON.
- **Mean bias**: Computed as the mean difference of the satellite measurements with TCCON.
- **"Relative systematic error"** (or "relative accuracy"): Computed as standard deviation of the biases as obtained at the various TCCON sites (computed for the entire time series of in additions seasonally resolved).
- **Stability: Linear bias trend (drift)**: Computed from the slope (and the error of the slope) as obtained by fitting a straight line to satellite minus TCCON differences.
- **Stability: Year-to-year bias variability**: Computed as maximum minus minimum bias difference of smoothed (using a one year running average) satellite minus TCCON differences.
- **QA/QC of the reported uncertainties**: The satellite-derived Level 2 XCO_2 and XCH_4 data products contain an uncertainty estimate for each single observation. This uncertainty is meant to be the statistical uncertainty (1-sigma) associated with that observation. To assess the quality of these uncertainty estimates they have been compared with the standard deviation of the satellite minus TCCON retrievals at the various TCCON sites. The ratio of the mean value of the reported uncertainty would be identical with the standard deviation of the difference to TCCON if the reported uncertainty is correct and if the comparison method does not introduce an additional error (which is typically not the case, e.g., due to imperfect co-location in time and space). Therefore, one expects that the ratio of the mean value of the reported uncertainty and the standard deviation of the satellite minus TCCON difference is close (i.e., within a few 10%) to unity and this been typically confirmed for all products.

For more details on how these metrics are calculated, the user is referred to the Main PQAR document, *Buchwitz et al., 2019*. To ensure comparable statistics, the TCCON stations used to calculate the relative systematic error and stability statistics are the same as those used in the analysis shown in the Main PQAR document.

2.1 Product CO2_GOS_OCFP

2.1.1 Validation

Figures 1 and 2 show a direct comparison of the co-located GOSAT and TCCON measurements over the entire temporal range of the dataset, as well as the results of a linear regression applied to the data. Figures 3 and 4 shows the GOSAT and TCCON data over each TCCON site, along with the mean bias and standard deviation (1-sigma). The average year-to-year stability (i.e. monthly mean TCCON-GOSAT bias smoothed using a 1 year running average) over all TCCON sites is plotted in Figures 5 and 6.

Figure 1: Correlation of TCCON GGG2014 and OCFPv7.3 XCO_2 observations over all TCCON sites mentioned in Table 2 (Radial co-location).

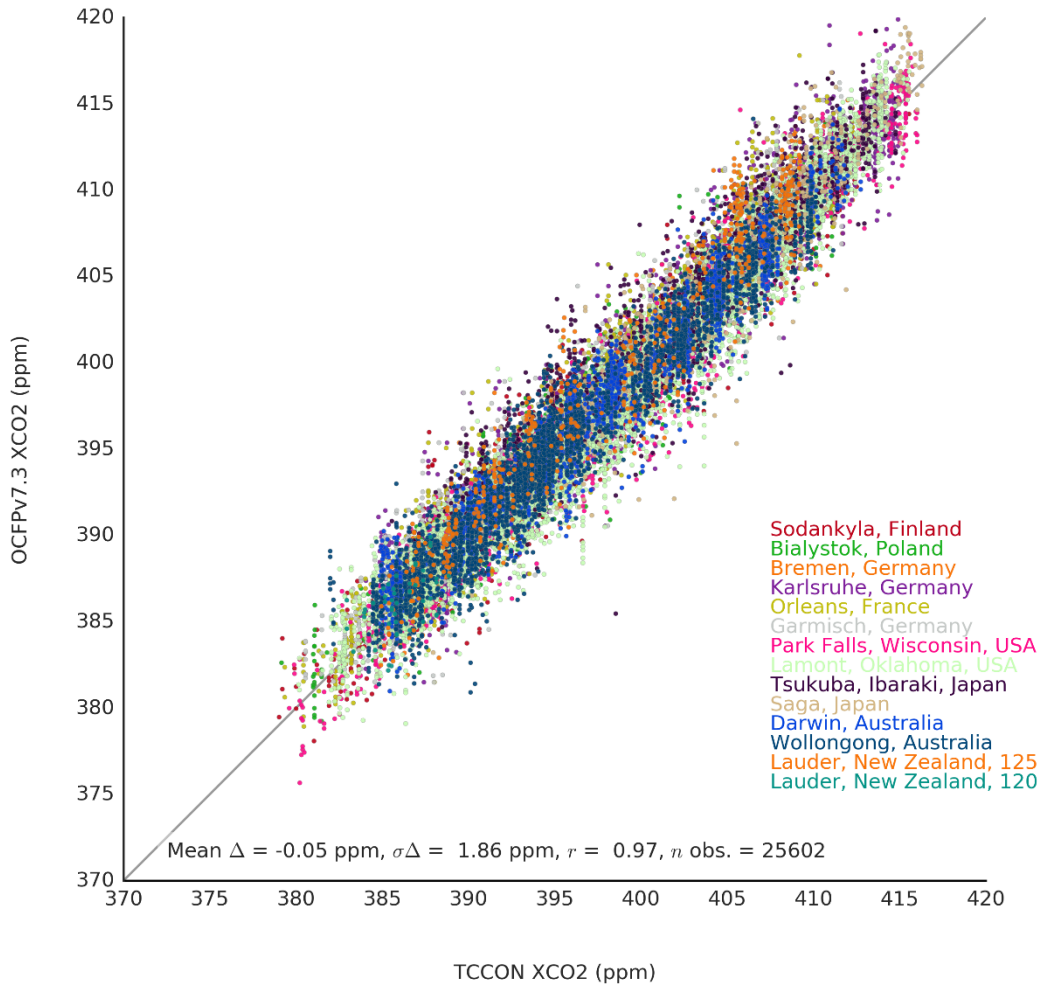

Figure 2: Correlation of TCCON GGG2014 and OCFPv7.3 XCO_2 observations over all TCCON sites mentioned in Table 2 (T700 co-location).

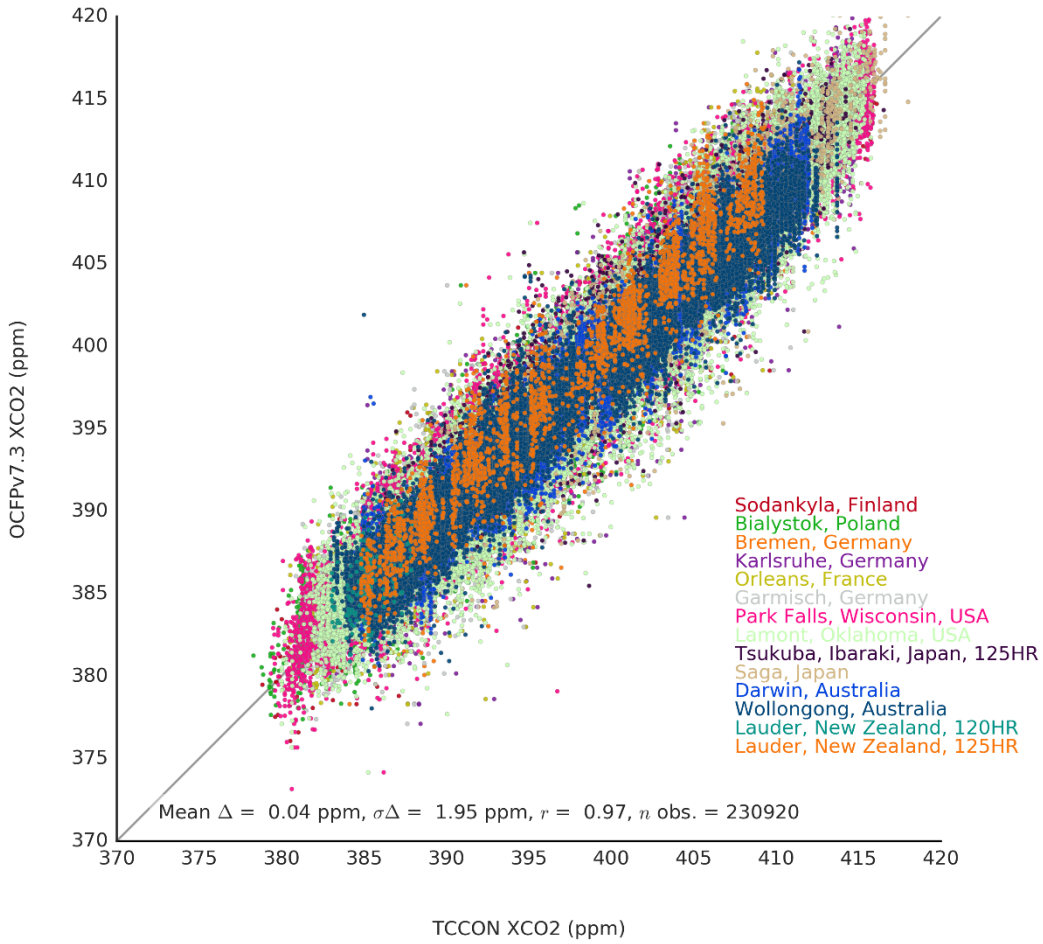

Figure 3: TCCON GGG2014 (green) and OCFPv7.3 (red) XCO_2 observations (Radial co-location).

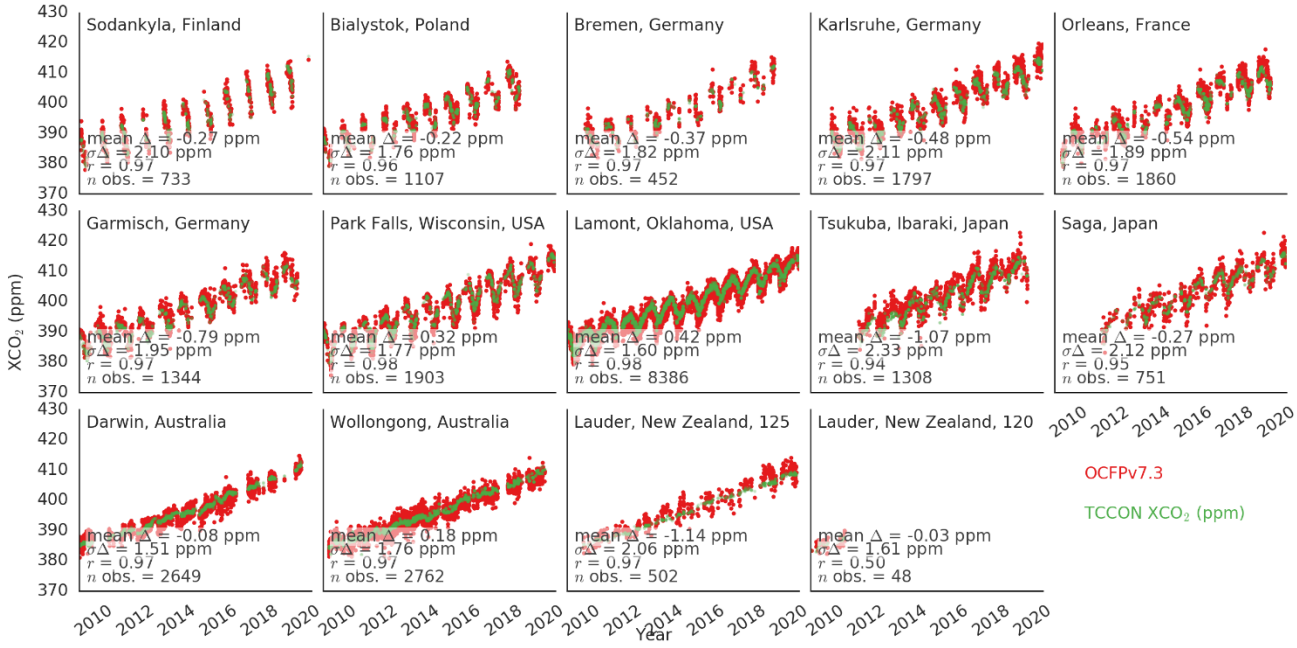

Figure 4: TCCON GGG2014 (green) and OCFPv7.3 (red) XCO_2 observations (T700 co-location).

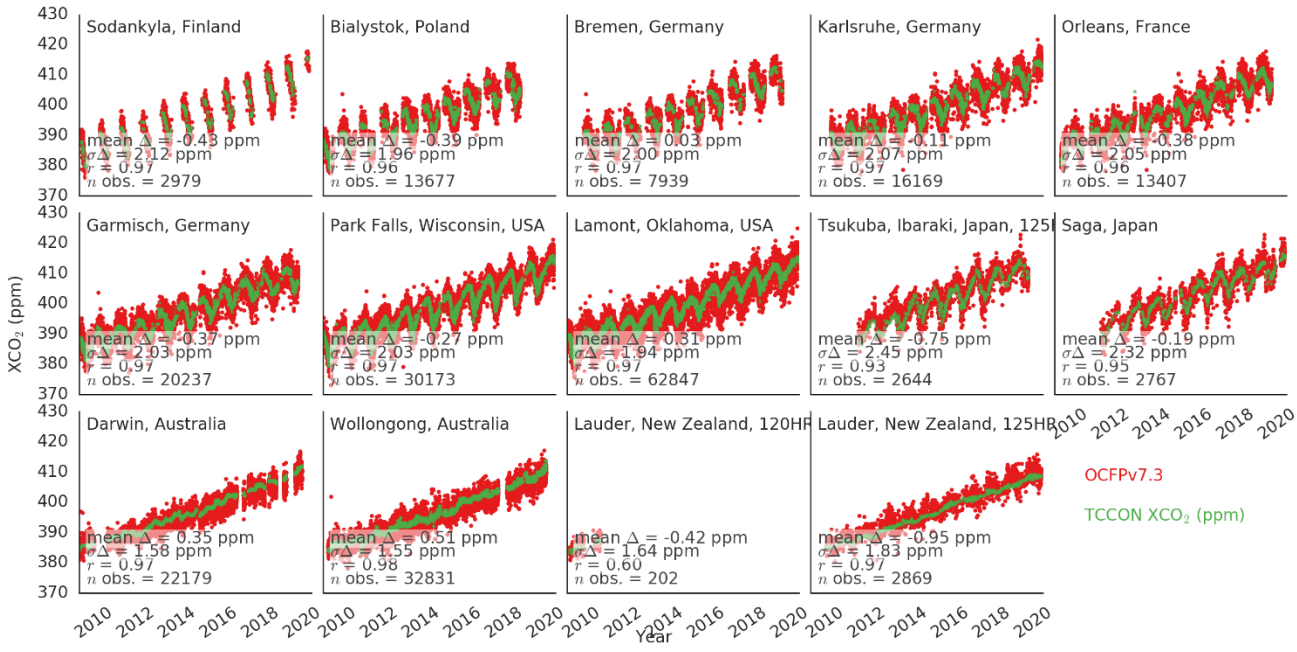

Figure 5: Year-to-year Stability of the TCCON-OCFPv7.3 XCO_2 bias calculated with ±6 month averaging window for each month of the GOSAT time series between April 2009 and June 2020, using the Radial co-location method. The thick blue symbols give the mean bias for a 12 month period and the shaded area indicates the standard deviation (1-sigma) of the data. The green lines give the number of data points per 12 month period.

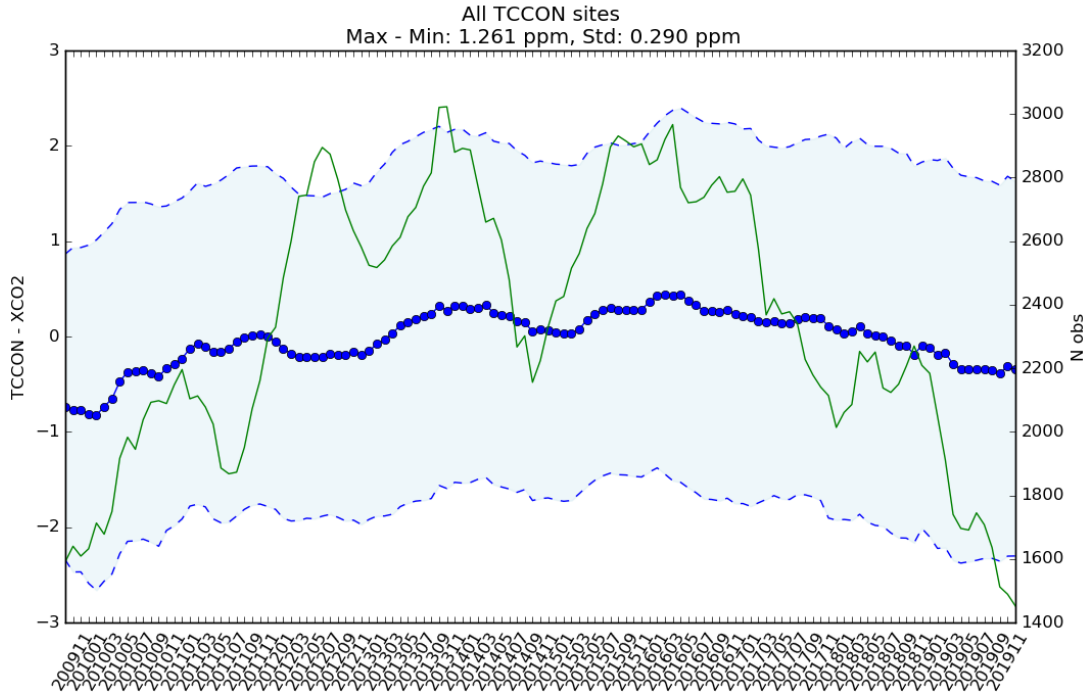

Figure 6: Year-to-year Stability of the TCCON-OCFPv7.3 XCO_2 bias calculated with ±6 month averaging window for each month of the GOSAT time series between April 2009 and June 2020, using the T700 co-location method. The thick blue symbols give the mean bias for a 12 month period and the shaded area indicates the standard deviation (1-sigma) of the data. The green lines give the number of data points per 12 month period.

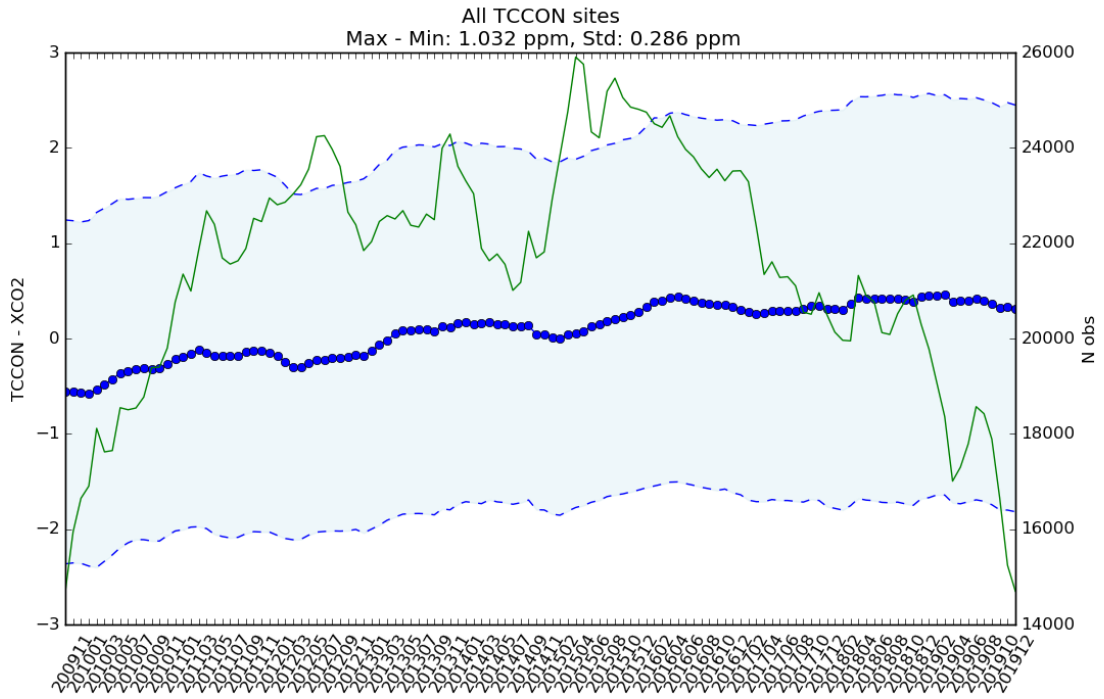

The derivation of the performance metrics discussed in Section 2 are discussed herein.

Single measurement precision

Table 3 shows the standard deviation of the TCCON-GOSAT bias recorded over each of the sites listed in Table 2. The mean single measurement precision over all sites was 1.90 ppm (1.99 ppm if using the T700 co-location method).

Table 3: The single measurement precision derived from the GOSAT-TCCON bias measured over each TCCON site listed in Table 2.

Site name	Single measurement precision (Radial method) [ppm]	Single measurement precision (T700 method) [ppm]
Sodankyla	2.10	2.12
Bialystok	1.76	1.96
Bremen	1.82	2.00
Karlsruhe	2.11	2.07
Orleans	1.89	2.05
Garmisch	1.95	2.03
Park Falls	1.77	2.03
Lamont	1.60	1.94
Tsukuba	2.33	2.45
Saga	2.12	2.32
Darwin	1.51	1.58
Wollongong	1.76	1.55
Lauder	2.06	1.83

Uncertainty ratio

To assess the quality of the reported XCO_2 uncertainty, these values are directly compared against the standard deviation of the TCCON-GOSAT bias. Ideally, the ratio of the reported GOSAT uncertainty against the TCCON-GOSAT bias should be close to unity. Table 4 shows the mean uncertainty ratio derived over each TCCON site. The mean uncertainty ratio was found to be 1.02 (0.96 if using the T700 co-location method), which suggests that the retrieved uncertainty is reliable for the CO2_GOS_OCFP product.

Table 4: The mean uncertainty ratio (measurement uncertainty: standard deviation of the TCCON-GOSAT bias) for each TCCON site listed in Table 2.

Site name	Uncertainty ratio (Radial method)	Uncertainty ratio (T700 method)
Sodankyla	1.03	1.01
Bialystok	1.14	1.00
Bremen	1.09	0.98
Karlsruhe	0.94	0.93
Orleans	1.01	0.93
Garmisch	1.02	0.95
Park Falls	1.08	0.97
Lamont	1.17	0.99
Tsukuba	0.93	0.84
Saga	1.00	0.90
Darwin	1.10	1.04
Wollongong	0.97	1.08
Lauder	0.80	0.88

Mean bias

The mean TCCON-GOSAT bias for each TCCON site is shown in Table 5. The mean bias over all sites is -0.05 ppm (0.04 ppm if using the T700 co-location method).

Table 5: The mean TCCON-GOSAT bias for each TCCON site listed in Table 2.

Site name	TCCON-GOSAT bias (Radial method) [ppm]	TCCON-GOSAT bias (T700 method) [ppm]
Sodankyla	-0.27	-0.43
Bialystok	-0.22	-0.39
Bremen	-0.37	0.03
Karlsruhe	-0.48	-0.11
Orleans	-0.54	-0.38
Garmisch	-0.79	-0.37
Park Falls	0.32	-0.27
Lamont	0.42	0.31
Tsukuba	-1.07	-0.75
Saga	-0.27	-0.19
Darwin	-0.08	0.35
Wollongong	0.18	0.51
Lauder	-1.14	-0.95

Relative systematic error

For this work the relative systematic error was computed as the standard deviation of the TCCON-GOSAT bias obtained at each TCCON site. In order to be consistent with past assessments, this was computed as two values:

- "Relative spatial bias": Standard deviation of the mean per-site bias computed over the entire time series
- "Relative spatio-temporal bias": Standard deviation of the seasonal mean bias at each TCCON site (i.e. JFM, AMJ, JJA, etc.)

The relative spatial bias can be directly calculated from the mean values listed in Table 5: 0.47 ppm (0.41 ppm if using the T700 co-location method).

Computation of the relative spatio-temporal bias requires sufficient co-located observations to occur throughout the year in order to calculate a seasonal average. For this work it was found that only the Darwin, Lamont, Park Falls, and Wollongong sites had sufficient observations to compute a seasonal average, which are shown in Table 6. The relative spatio-temporal bias was calculated as the mean of these values: 0.80 ppm (0.64 ppm if using the T700 co-location method).

Table 6: The relative spatio-temporal bias (standard deviation of the seasonal mean bias) for each TCCON site listed in Table 2, over which sufficient observations were recorded over all seasons.

Site name	Relative spatio-temporal bias (Radial method) [ppm]	Relative spatio-temporal bias (T700 method) [ppm]
Darwin	0.98	0.73
Lamont	0.72	0.60
Park Falls	0.85	0.67
Wollongong	0.64	0.56

Stability (Linear drift)

For each TCCON site, the linear drift was calculated as the slope of the linear regression of the daily mean TCCON-GOSAT bias against time. The slope fit error was also calculated in order to give the 1-sigma uncertainty. The sites shown in Table 6 were found to have a sufficient number of observations to compute a robust drift estimate. Table 7 shows the drift and error calculated for these sites. The mean drift over these stations is: 0.10 ± 0.04ppm/year (0.10 ± 0.03 ppm/year if using the T700 co-location method)

Table 7: The linear drift and 1-sigma uncertainty calculated for each site listed in Table 2, over which sufficient observations were recorded over the entire time period.

Site name	Linear drift (Radial method) [ppm/year]	Linear drift (T700 method) [ppm/year]
Darwin	0.19 ± 0.02	0.14 ± 0.01
Lamont	0.03 ± 0.01	0.05 +/- 0.01
Park Falls	0.04 ± 0.02	0.06 ± 0.01
Wollongong	0.14 ± 0.02	0.16 ± 0.01

Stability (year-to-year bias variability)

For all TCCON sites the year-to-year variability was calculated by first computing a monthly mean of the TCCON-GOSAT bias. To minimise the influence of monthly variations, a one year (12 months) running average was applied to the time series. Finally, the year-to-year variability is taken as the difference between the minimum and maximum value. Figures 5 and 6 show the smoothed monthly mean bias derived using this method, as well as the mean and standard deviation of the year-to-year stability derived from all TCCON sites.

2.1.2 Validation summary

The validation results are summarized in the tables below.

Table 8 - Product Quality Summary Table for product CO2_GOS_OCFP (Radial co-location).

Product Quality Summary Table for Product: CO2_GOS_OCFP Level: 2, Version: 7.3, Time period covered: 4.2009 – 6.2020				
Parameter [unit]	Achieved performance	Requirement	TR	Comments
Single measurement precision (1-sigma) in [ppm]	1.90	< 8 (T) < 3 (B) < 1 (G)	-	-
Uncertainty ratio in [-]: Ratio reported uncertainty to standard deviation of satellite-TCCON difference	1.02	-	-	No requirement but value close to unity expected for a high quality data product.
Mean bias [ppm]	-0.05	-	-	No requirement but value close to zero expected for a high quality data product.
Accuracy: Relative systematic error [ppm]	Spatial – spatiotemporal: 0.47 – 0.80	< 0.5	Probability that accuracy TR is met: 35%	-
Stability: Drift [ppm/year]	0.10 ± 0.04 (1-sigma)	< 0.5	Probability that stability TR is met: 97%	-
Stability: Year-to-year bias variability [ppm/year]	1.26 ± 0.29 (1-sigma)	< 0.5	-	-

Table 9 - Product Quality Summary Table for product CO2_GOS_OCFP (T700 co-location).

Product Quality Summary Table for Product: CO2_GOS_OCFP Level: 2, Version: 7.3, Time period covered: 4.2009 – 6.2020				
Parameter [unit]	Achieved performance	Requirement	TR	Comments
Single measurement precision (1-sigma) in [ppm]	1.99	< 8 (T) < 3 (B) < 1 (G)	-	-
Uncertainty ratio in [-]: Ratio reported uncertainty to standard deviation of satellite-TCCON difference	0.96	-	-	No requirement but value close to unity expected for a high quality data product.
Mean bias [ppm]	0.04	-	-	No requirement but value close to zero expected for a high quality data product.
Accuracy: Relative systematic error [ppm]	Spatial – spatiotemporal: 0.41 – 0.64	< 0.5	Probability that accuracy TR is met: 55%	-
Stability: Drift [ppm/year]	0.10 +/- 0.03 (1-sigma)	< 0.5	Probability that stability TR is met: 96%	-
Stability: Year-to-year bias variability [ppm/year]	1.03 ± 0.29 (1-sigma)	< 0.5	-	-

2.2 Product CH4_GOS_OCFP

2.2.1 Validation

Similar figures as shown in 2.1.1 for product CO2_GOS_OCFP are shown in this section but for the product CH4_GOS_OCFP.

Figure 7: Correlation of TCCON GGG2014 and OCFPv7.3 XCH_4 observations over all TCCON sites mentioned in Table 2.

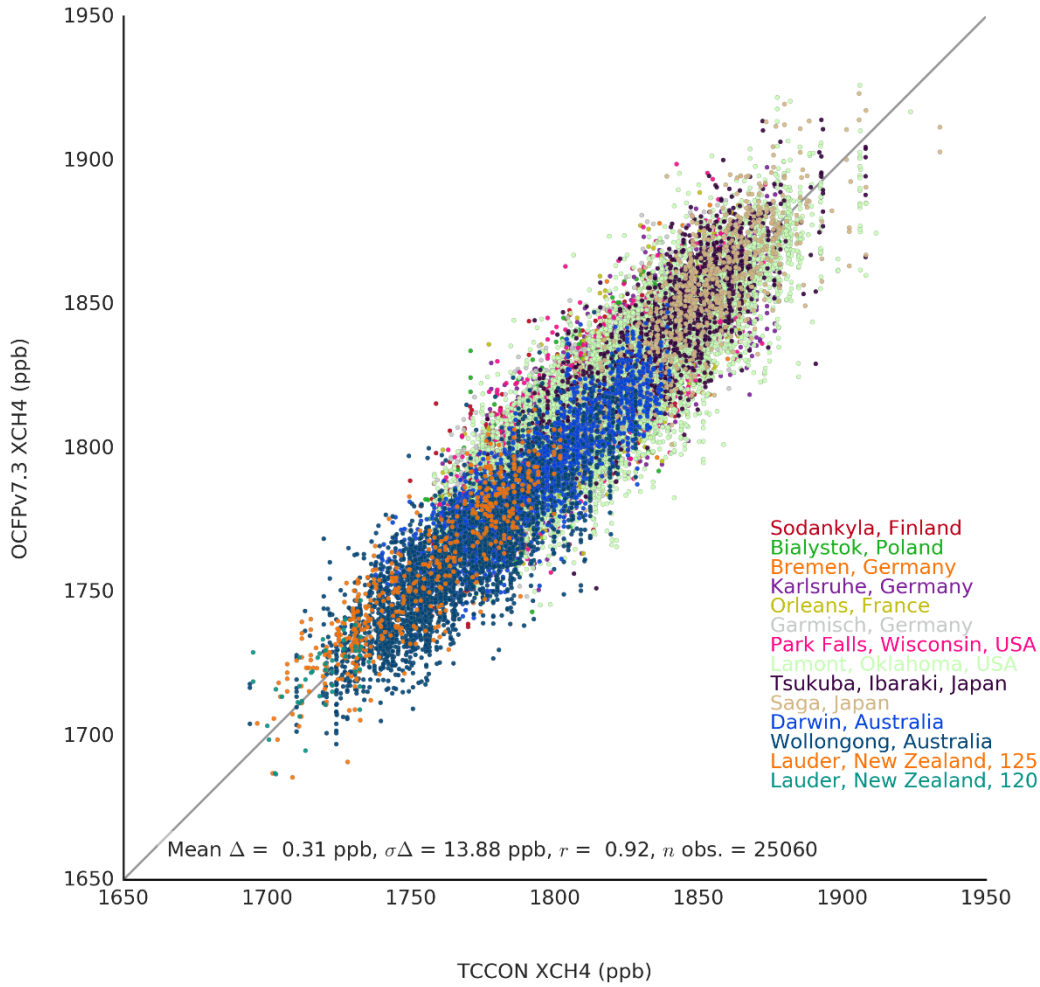

Figure 8: TCCON GGG2014 (green) and OCFPv7.3 (red) XCH_4 observations; OCFP observations are co-located with TCCON sites using a 555 km spatial and a ±2 hour temporal criteria.

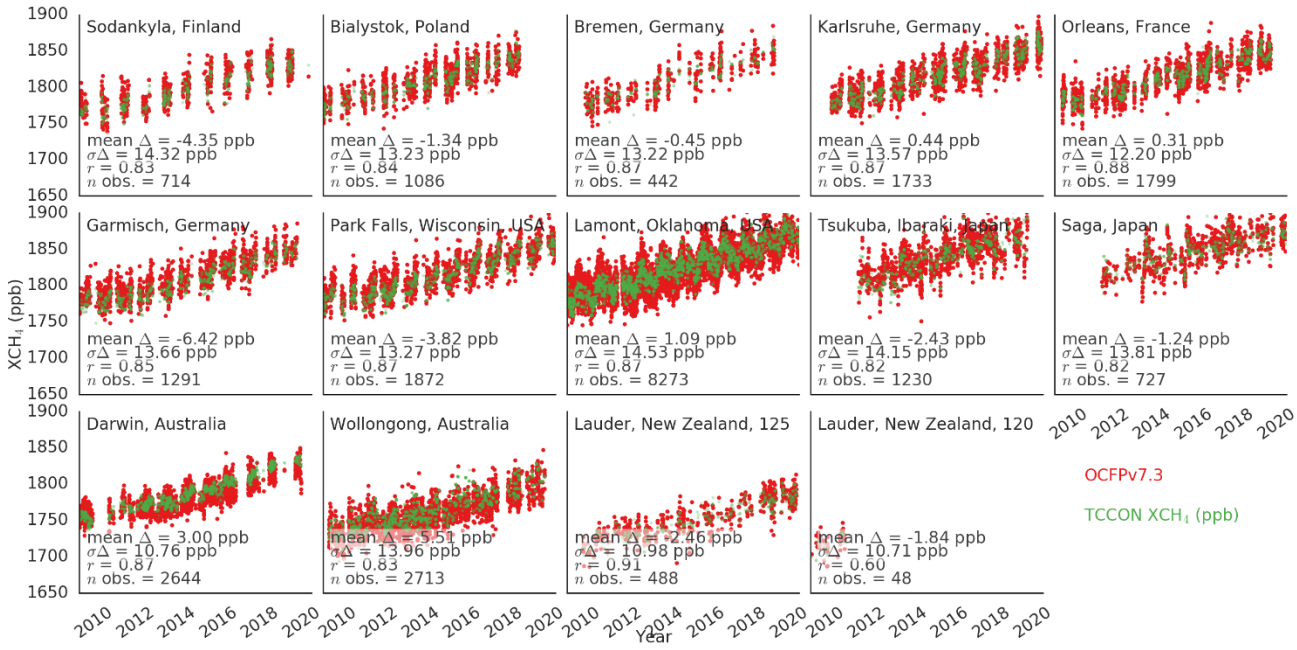

Figure 9: Year-to-year Stability of the TCCON-OCFPv7.3 XCH_4 bias calculated with for ±6 month averaging window for each month of the GOSAT time series between April 2009 and June 2020. The thick blue symbols give the mean bias for a 12 month period and the shaded area indicates the standard deviation (1-sigma) of the data. The green lines gives the number of data points per 12 month period.

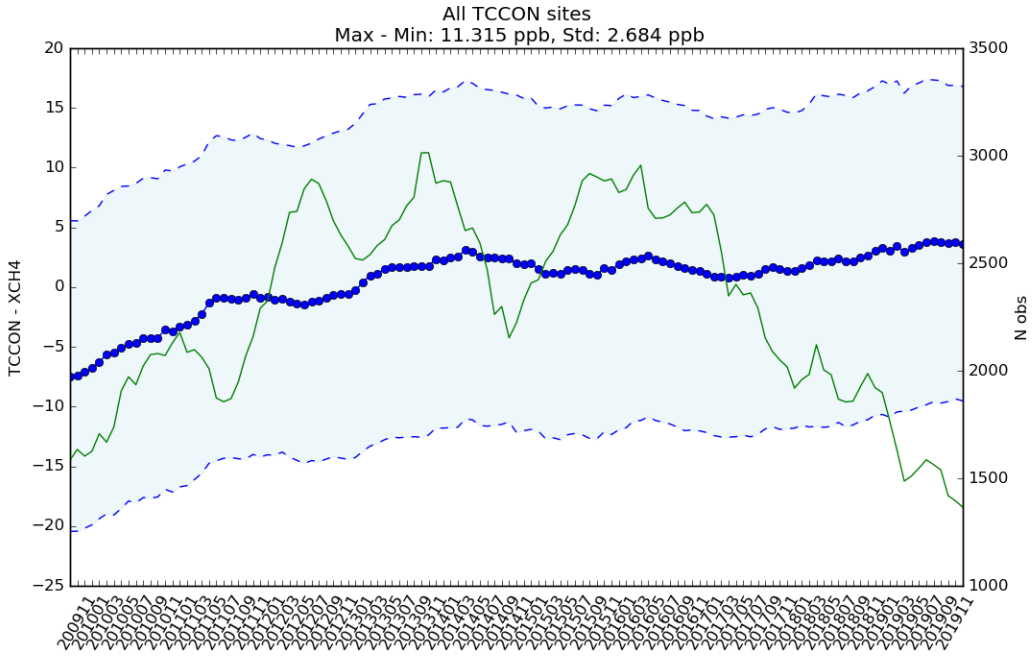

As in Section 2.1.1, the calculation of the validation metrics are discussed herein.

Single measurement precision

Table 10 shows the standard deviation of the TCCON-GOSAT bias recorded over each of the sites listed in Table 2. The mean single measurement precision over all sites was 13.20 ppb.

Table 10: The single measurement precision derived from the GOSAT-TCCON bias measured over each TCCON site listed in Table 2.

Site name	Single measurement precision [ppb]
Sodankyla	14.32
Bialystok	13.23
Bremen	13.22
Karlsruhe	13.57
Orleans	12.20
Garmisch	13.66
Park Falls	13.27
Lamont	14.53
Tsukuba	14.15
Saga	13.81
Darwin	10.76
Wollongong	13.96
Lauder	10.98

Uncertainty ratio

Table 11 shows the mean uncertainty ratio derived over each TCCON site. The mean uncertainty ratio was found to be 1.09, which suggests that the retrieved uncertainty is reliable for the CH4_GOS_OCFP product.

Table 11: The mean uncertainty ratio (measurement uncertainty: standard deviation of the TCCON-GOSAT bias) for each TCCON site listed in Table 2.

Site name	Uncertainty ratio
Sodankyla	1.11
Bialystok	1.11
Bremen	1.14
Karlsruhe	1.08
Orleans	1.19
Garmisch	1.08
Park Falls	1.07
Lamont	0.94
Tsukuba	1.09
Saga	1.06
Darwin	1.14
Wollongong	0.94
Lauder	1.18

Mean bias

The mean TCCON-GOSAT bias for each TCCON site is shown in Table 12. The mean bias over all sites is 0.31 ppb.

Table 12: The mean TCCON-GOSAT bias for each TCCON site listed in Table 2.

Site name	TCCON-GOSAT bias [ppb]
Sodankyla	-4.35
Bialystok	-1.34
Bremen	-0.45
Karlsruhe	0.44
Orleans	0.31
Garmisch	-6.42
Park Falls	-3.82
Lamont	1.09
Tsukuba	-2.43
Saga	-1.24
Darwin	3.00
Wollongong	5.51
Lauder	-2.46

Relative systematic error

The relative spatial bias can be directly calculated from the mean values listed in Table 12: 3.03 ppb.

Computation of the relative spatio-temporal bias requires sufficient co-located observations to occur throughout the year in order to calculate a seasonal average. For this work it was found that only the Darwin, Lamont, Park Falls, and Wollongong sites had sufficient observations to compute a seasonal average, which are shown in Table 13. The relative spatio-temporal bias was calculated as the mean of these values: 6.20 ppb.

Table 13: The relative spatio-temporal bias (standard deviation of the seasonal mean bias) for each TCCON site listed in Table 2, over which sufficient observations were recorded over all seasons.

Site name	Relative spatio-temporal bias [ppb]
Darwin	5.50
Lamont	6.04
Park Falls	7.77
Wollongong	5.47

Stability (Linear drift)

The sites shown in Table 13 were found to have a sufficient number of observations to compute a robust drift estimate. Table 14 shows the drift and error calculated for these sites. The mean drift over these stations is: 0.96 ± 0.20 ppb/year

Table 14: The linear drift and 1-sigma uncertainty calculated for each site listed in Table 2, over which sufficient observations were recorded over the entire time period.

Site name	Linear drift [ppb/year]
Darwin	1.39± 0.13
Lamont	1.09 ± 0.12
Park Falls	0.78 ± 0.16
Wollongong	0.58 ± 0.18

Stability (year-to-year bias variability)

Figure 9 shows the smoothed monthly mean bias derived using this method, as well as the mean and standard deviation of the year-to-year stability derived from all TCCON sites.

2.2.2 Validation summary

The validation results are summarized in the table below.

Table 15 - Product Quality Summary Table for product CH4_GOS_OCFP.

Product Quality Summary Table for Product: CH4_GOS_OCFP Level: 2, Version: 7.3, Time period covered: 4.2009 – 6.2020				
Parameter [unit]	Achieved performance	Requirement	TR	Comments
Single measurement precision (1-sigma) in [ppb]	13.20	< 34 (T) < 17 (B) < 9 (G)	-	-
Uncertainty ratio in [-]: Ratio reported uncertainty to standard deviation of satellite-TCCON difference	1.09	-	-	No requirement but value close to unity expected for a high quality data product.
Mean bias [ppb]	0.31	-	-	No requirement but value close to zero expected for a high quality data product.
Accuracy: Relative systematic error [ppb]	Spatial – spatiotemporal: 3.03– 6.20	< 10	Probability that accuracy TR is met: 84%	-
Stability: Linear bias trend [ppb/year]	0.96 ± 0.20 (1-sigma)	< 3	Probability that stability TR is met: 97%	-
Stability: Year-to-year bias variability [ppb/year]	11.32 ± 2.68 (1-sigma)	< 3	-	-

2.3 Product CH4_GOS_OCPR

2.3.1 Validation

Similar figures as shown in 2.1.1 for product CO2_GOS_OCFP are shown in this section but for the product CH4_GOS_OCPR.

Figure 10: Correlation of TCCON GGG2014 and OCPRv9.0 XCH_4 observations over all TCCON sites mentioned in Table 2.

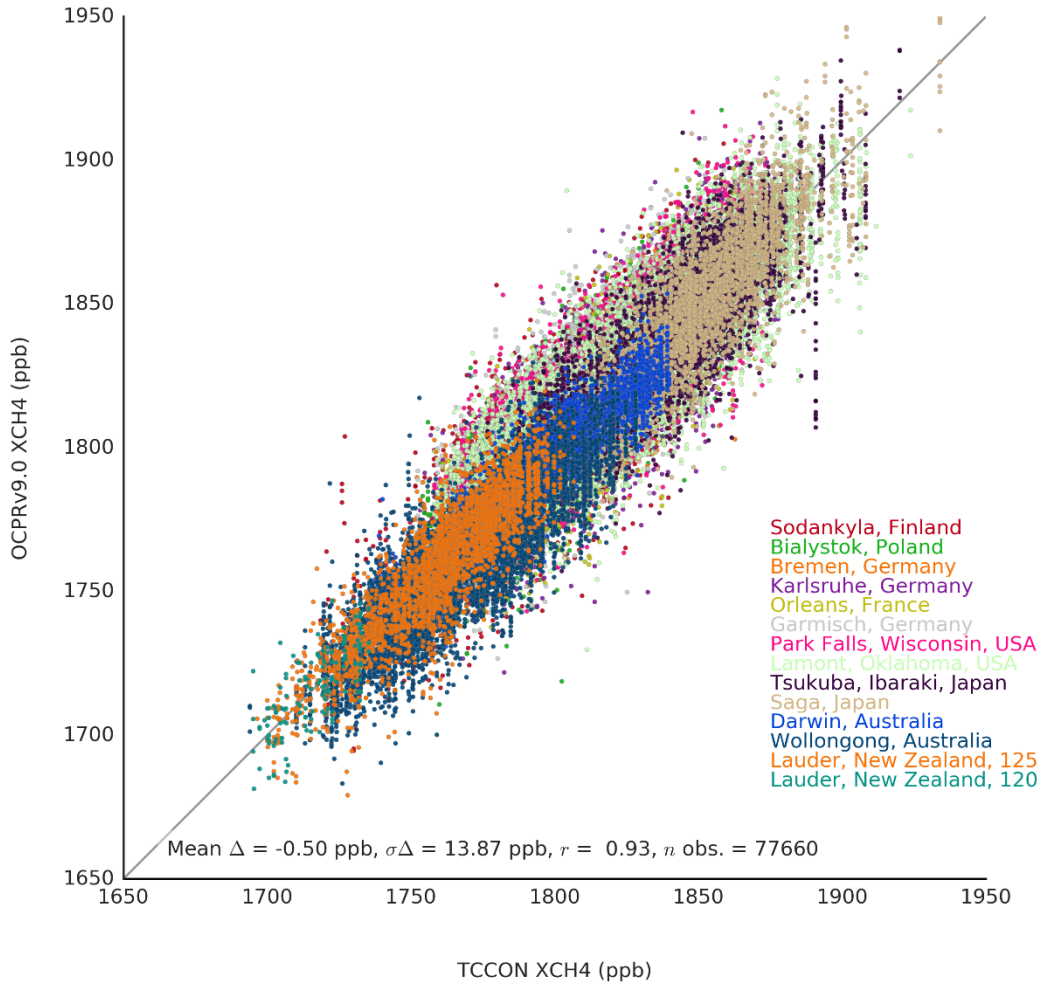

Figure 11: TCCON GGG2014 (green) and OCPRv9.0 (red) XCH_4 observations; OCPR observations are co-located with TCCON sites using a 555 km spatial and a ±2 hour temporal criterion.

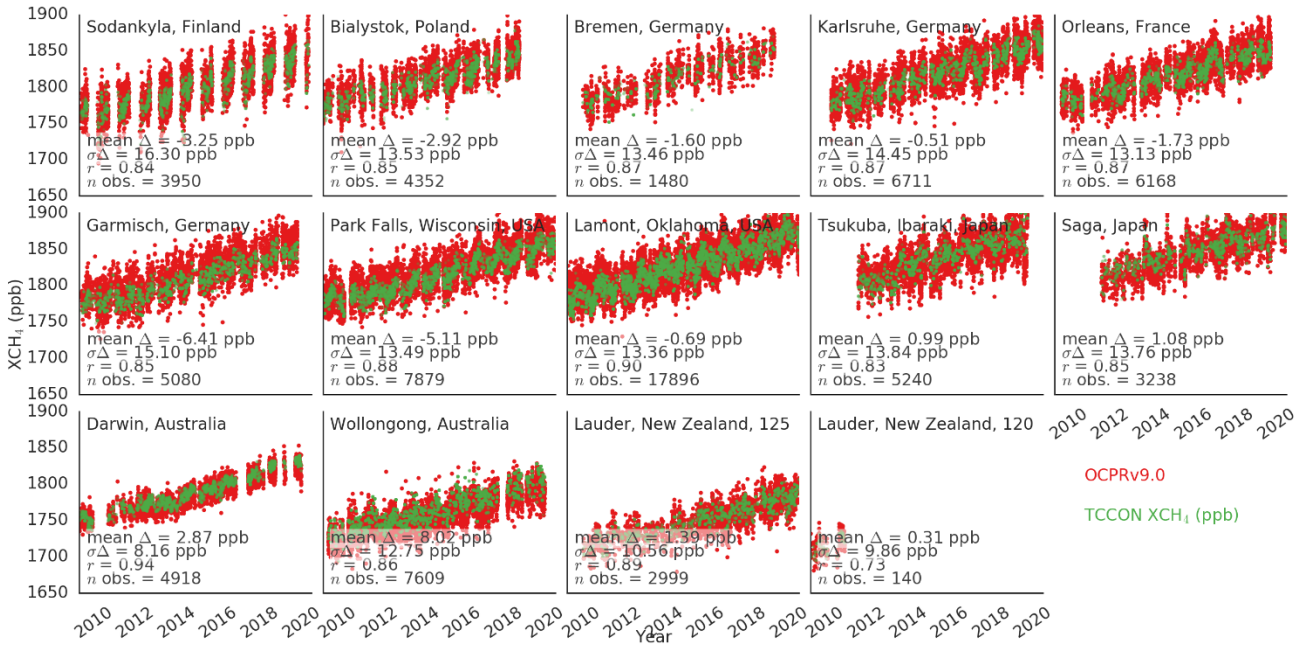

Figure 12: Year-to-year Stability of the TCCON-OCPRv9.0 XCH_4 bias calculated with ±6 month averaging window for each month of the GOSAT time series between April 2009 and June 2020. The thick blue symbols give the mean bias for a 12 month period and the shaded area indicates the standard deviation (1-sigma) of the data. The green lines gives the number of data points per 12 month period.

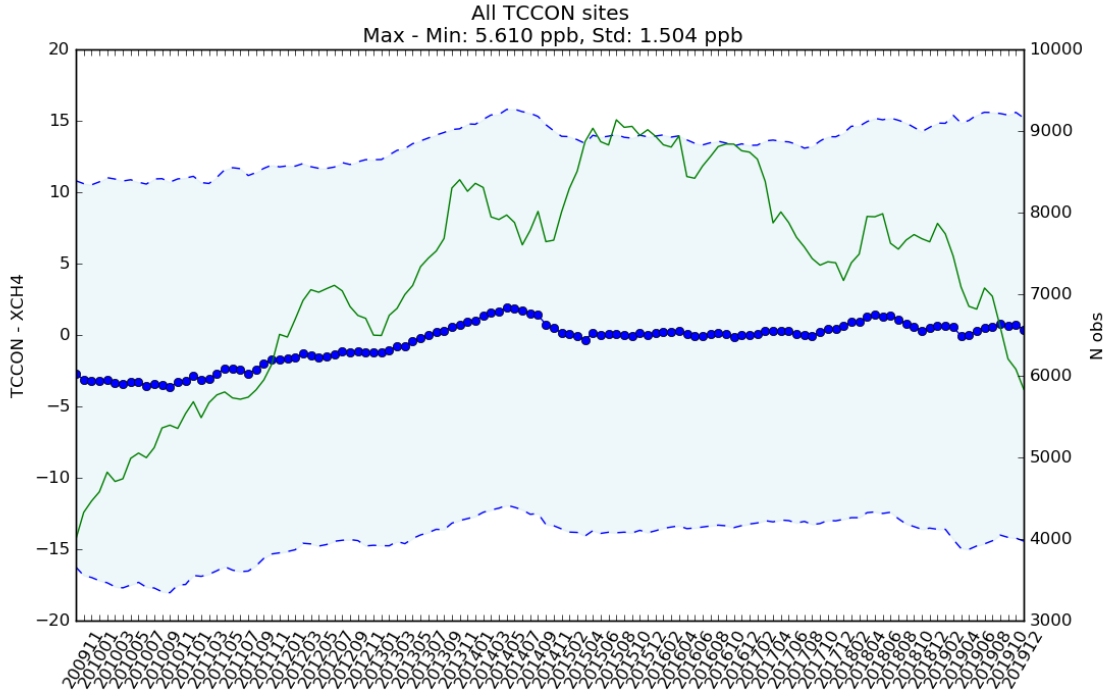

As in Section 2.1.1, the calculation of the validation metrics are discussed herein.

Single measurement precision

Table 16 shows the standard deviation of the TCCON-GOSAT bias recorded over each of the sites listed in Table 2. The mean single measurement precision over all sites was 13.20 ppb.

Table 16: The single measurement precision derived from the GOSAT-TCCON bias measured over each TCCON site listed in Table 2.

Site name	Single measurement precision [ppb]
Sodankyla	14.32
Bialystok	13.23
Bremen	13.22
Karlsruhe	13.57
Orleans	12.20
Garmisch	13.66
Park Falls	13.27
Lamont	14.53
Tsukuba	14.15
Saga	13.81
Darwin	10.76
Wollongong	13.96
Lauder	10.98

Uncertainty ratio

Table 17 shows the mean uncertainty ratio derived over each TCCON site. The mean uncertainty ratio was found to be 0.83, which suggests that the retrieved uncertainty is reliable for the CH4_GOS_OCPR product.

Table 17: The mean uncertainty ratio (measurement uncertainty: standard deviation of the TCCON-GOSAT bias) for each TCCON site listed in Table 2.

Site name	Uncertainty ratio
Sodankyla	0.76
Bialystok	0.84
Bremen	0.84
Karlsruhe	0.78
Orleans	0.85
Garmisch	0.75
Park Falls	0.85
Lamont	0.78
Tsukuba	0.82
Saga	0.78
Darwin	1.14
Wollongong	0.72
Lauder	0.91

Mean bias

The mean TCCON-GOSAT bias for each TCCON site is shown in Table 18. The mean bias over all sites is 0.31 ppb.

Table 18: The mean TCCON-GOSAT bias for each TCCON site listed in Table 2.

Site name	TCCON-GOSAT bias [ppb]
Sodankyla	-4.35
Bialystok	-1.34
Bremen	-0.45
Karlsruhe	0.44
Orleans	0.31
Garmisch	-6.42
Park Falls	-3.82
Lamont	1.09
Tsukuba	-2.43
Saga	-1.24
Darwin	3.00
Wollongong	5.51
Lauder	-2.46

Relative systematic error

The relative spatial bias can be directly calculated from the mean values listed in Table 18: 3.03 ppb.

Computation of the relative spatio-temporal bias requires sufficient co-located observations to occur throughout the year in order to calculate a seasonal average. For this work it was found that only the following sites had sufficient observations to compute a seasonal average (see Table 19): Bialystok, Darwin, Garmisch, Karlsruhe, Lauder, Lamont, Park Falls, Saga, Sodankyla, and Wollongong. The relative spatio-temporal bias was calculated as the mean of these values: 4.42 ppb.

Table 19: The relative spatio-temporal bias (standard deviation of the seasonal mean bias) for each TCCON site listed in Table 2, over which sufficient observations were recorded over all seasons.

Site name	Relative spatio-temporal bias [ppb]
Bialystok	3.98
Darwin	3.40
Garmisch	4.13
Karlsruhe	5.61
Lauder	3.57
Lamont	4.33
Park Falls	3.03
Saga	5.26
Sodankyla	5.58
Wollongong	5.28

Stability (Linear drift)

The sites shown in Table 19 were found to have a sufficient number of observations to compute a robust drift estimate. Table 20 shows the drift and error calculated for these sites. The mean drift over these stations is: 0.15 ± 0.56 ppb/year

Table 20: The linear drift and 1-sigma uncertainty calculated for each site listed in Table 2, over which sufficient observations were recorded over the entire time period.

Site name	Linear drift [ppb/year]
Bialystok	0.09 ± 0.15
Darwin	0.63 ± 0.08
Garmisch	0.02 +/- 0.14
Karlsruhe	0.45 +/- 0.12
Lauder	0.14 ± 0.11
Lamont	0.91 ± 0.09
Park Falls	0.18 ± 0.09
Saga	-1.32± 0.19
Sodankyla	-0.09 +/- 0.15
Wollongong	0.50 ± 0.13

Stability (year-to-year bias variability)

Figure 12 shows the smoothed monthly mean bias derived using this method, as well as the mean and standard deviation of the year-to-year stability derived from all TCCON sites.

2.3.2 Validation summary

The validation results are summarized in the table below.

Table 21 - Product Quality Summary Table for product CH4_GOS_OCPR.

Product Quality Summary Table for Product: CH4_GOS_OCPR Level: 2, Version: 9.0, Time period covered: 4.2009 – 6.2020				
Parameter [unit]	Achieved performance	Requirement	TR	Comments
Single measurement precision (1-sigma) in [ppb]	13.20	< 34 (T) < 17 (B) < 9 (G)	-	-
Uncertainty ratio in [-]: Ratio reported uncertainty to standard deviation of satellite-TCCON difference	0.83	-	-	No requirement but value close to unity expected for a high quality data product.
Mean bias [ppb]	0.31	-	-	No requirement but value close to zero expected for a high quality data product.
Accuracy: Relative systematic error [ppb]	Spatial – spatiotemporal: 3.03 – 4.42	< 10	Probability that accuracy TR is met: 90%	-
Stability: Linear bias trend [ppb/year]	0.15 ± 0.56 (1-sigma)	< 3	Probability that stability TR is met: 99%	-
Stability: Year-to-year bias variability [ppb/year]	5.61 ± 1.50 (1-sigma)	< 3	-	-

3. Application(s) specific assessments

In addition to TCCON, the UoL C3S products can also be compared with XCO_2 and XCH_4, modelled by the CarbonTracker (2019 + NRT-2020) and MACC S1NOAAv10 datasets, respectively. However, these datasets do not cover the entire temporal range of the GOSAT measurements; CarbonTracker data is available up to mid-2019, while MACC S1NOAAv10 is only available up to 2012. At the time of writing this report, CarbonTracker data for 2020 were not yet available. It should also be noted that for MACC S1NOAAv10 the stratospheric profile has been replaced with calculations from the TOMCAT model. The modelled CO_2 and CH_4 vertical profiles were convolved with the GOSAT averaging kernel before being compared with the UoL products.

Figure 13 shows the seasonal mean difference between the OCFP and CarbonTracker XCO_2. The lack of significant biases (i.e. more than ±3 ppm) suggest that the magnitudes of the OCFP data are in line with expected values. Large seasonal biases are observed in Central-Eastern Asia and the Sahara, potentially due to pyrogenic emissions unaccounted for in the model, or the occurrence of high aerosol loadings unaccounted for by the retrieval.

Figure 14 shows the seasonal mean difference between the OCFP and MACC and TOMCAT XCH_4. As with CO_2, no significant differences (i.e. more than ±50 ppm) were observed anywhere on the globe. Larger differences occur over South America in spring and summer and over Arabian Peninsula and North-Eastern Africa in summer, potentially because of higher than expected aerosol loading.

Figure 15 shows the seasonal mean difference between the OCPR and MACC and TOMCAT XCH_4. Significantly large negative biases are observed over Tibet, potentially due to aerosol loading or surface elevation that is unaccounted for in the retrieval. Aside from this, the results appear in line with the OCFP dataset, as no significantly large biases are observed, though regions where fluxes are uncertain (e.g. South-East Asia in autumn or southern Africa in winter) show higher than background differences with the model data.

Figure 13: Seasonal means of differences between OCFPv7.3 and CarbonTracker (2019 + NRT-2020) XCO_2.

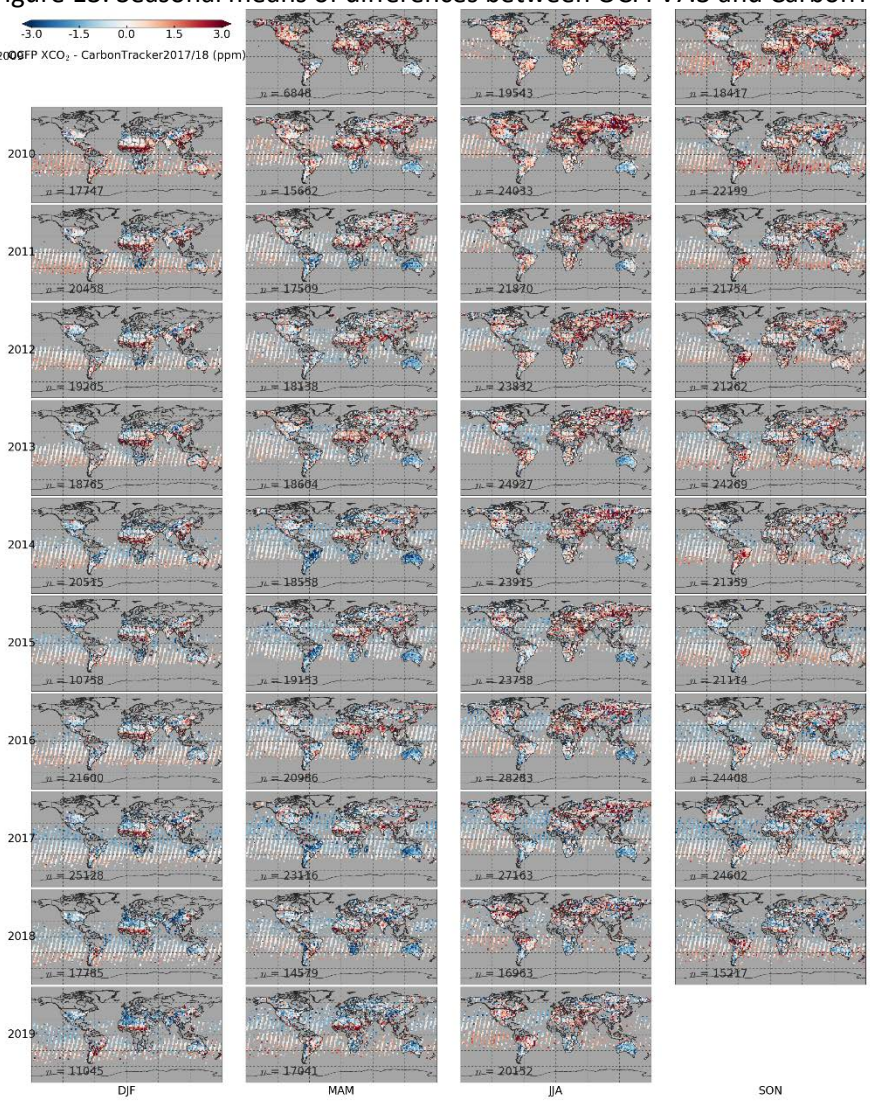

Figure 14: Seasonal means of differences between OCFP7.3 and MACC S1NOAAv10 + TOMCAT XCH_4.

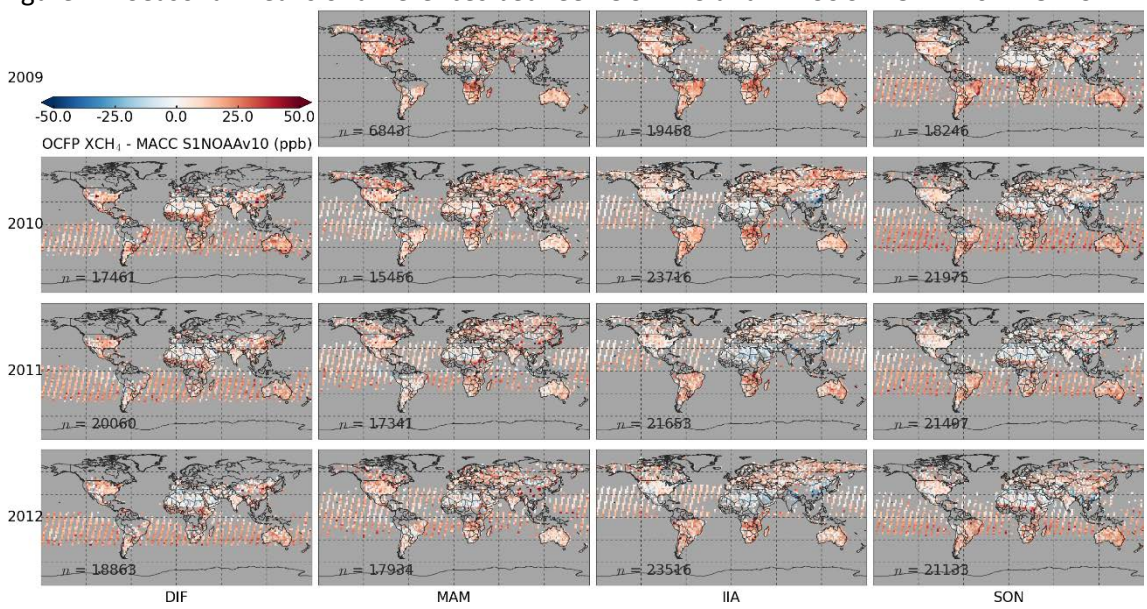

Figure 15: Seasonal means of differences between OCPRv9.0 and MACC S1NOAAv10 + TOMCAT XCH_4.

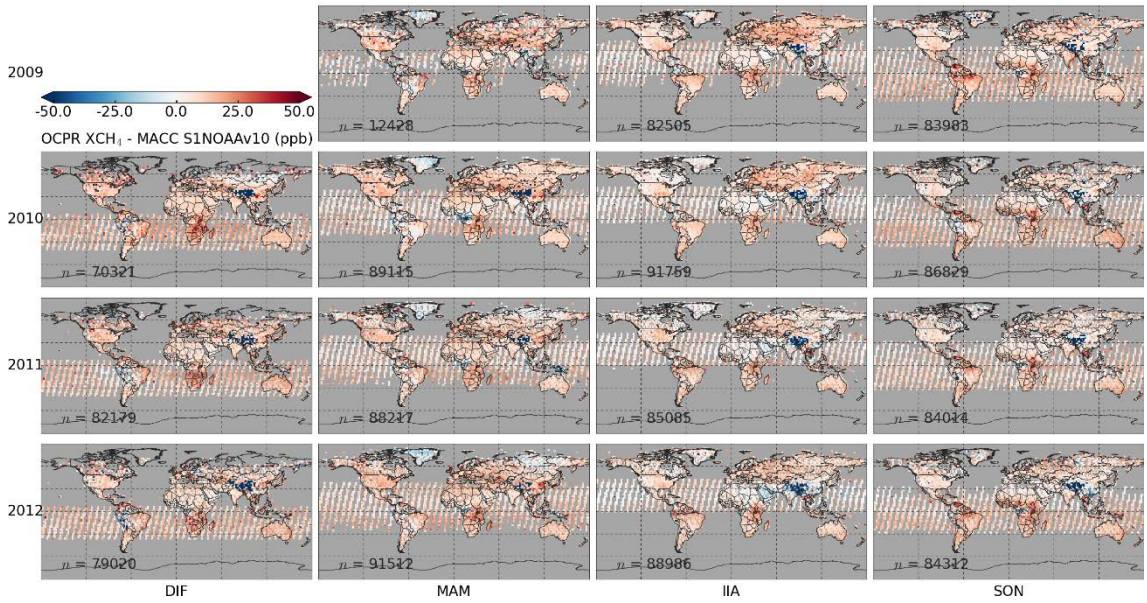

4. Compliance with user requirements

The results in Section 2.1.2, 2.2.2, and 2.3.2 show the probability that the TR for relative accuracy and linear bias trend (stability) are met for each product. For CH_4, the OCFP and OCPR products show a very high likelihood that these requirements are met. However, the CO_2 product shows a low probability of meeting the relative accuracy requirement (37 or 55% depending on the co-location criterion, see Tables 8-9), though it manages to meet the linear bias trend stability requirement. All products have difficulties meeting the year-to-year stability requirement.

References

Boesch et al., 2011: Boesch, H., D. Baker, B. Connor, D. Crisp, and C. Miller, Global characterization of CO_2 column retrievals from shortwave-infrared satellite observations of the Orbiting Carbon Observatory-2 mission, Remote Sensing, 3 (2), 270-304, 2011.

Boesch et al., 2019: Boesch, H., Anand, J., and Di Noia, A.: Algorithm Theoretical Basis Document (ATBD) – ANNEX A for products CO2_GOS_OCFP, CH4_GOS_OCFP & CH4_GOS_OCPR (v7.2, 2009-2018), project C3S_312b_Lot2_DLR – Atmosphere, v3.1, 2019.

Buchwitz et al., 2019: Buchwitz, M., Reuter, M., Schneising-Weigel, O., Aben, I., Detmers, R. G., Hasekamp, O. P., Boesch, H., Anand, J., Di Noia, A., Crevoisier, C., and Armante, R.: Product Quality Assessment Report (PQAR) – Main document for Greenhouse Gas (GHG: CO2 & CH4) data set CDR 3 (2003-2018), project C3S_312b_Lot2_DLR – Atmosphere, v3.1, 2019.

Butz et al., 2010: Butz, A., Hasekamp, O. P., Frankenberg, C., Vidot, J. and Aben, I.: CH4 retrievals from space-based solar backscatter measurements: Performance evaluation against simulated aerosol and cirrus loaded scenes, J. Geophys. Res., 115(D24), doi:10.1029/2010JD014514, 2010.

Chevallier et al., 2010: Chevallier, F., Feng, L., Boesch, H. Palmer, P., and Rayner, P., On the impact of transport model errors for the estimation of CO_2 surface fluxes from GOSAT observations, Geophys. Res. Let., 37, L21803, 2010.

Frankenberg et al., 2011: Frankenberg, C., Aben, I., Bergamaschi, P., et al., Global column-averaged methane mixing ratios from 2003 to 2009 as derived from SCIAMACHY: Trends and variability, *J. Geophys. Res*., doi:10.1029/2010JD014849, 2011.

Hollmann et al., 2013: Hollmann, C.J. Merchant, R. Saunders, C. Downy, M. Buchwitz, A. Cazenave, E. Chuvieco, P. Defourny, G. de Leeuw, R. Forsberg, T. Holzer-Popp, F. Paul, S. Sandven, S. Sathyendranath, M. van Roozendael, W. Wagner, The ESA Climate Change Initiative: satellite data records for essential climate variables, Bulletin of the American Meteorological Society (BAMS), 0.1175/BAMS-D-11-00254.1, pp. 12, 2013.

O'Dell, 2010: O'Dell, C. W.: Acceleration of multiple-scattering, hyper-spectral radiative transfer calculations via low-streams interpolation, Journal of Geophysical Research D: Atmospheres, 115(10), 2010.

Peters et al., 2007: Peters, W., Jacobson, A. R., Sweeney, C., Andrews, A. E., Conway, T. J., Masarie, K., Miller, J. B., Bruhwiler, L. M. P., Petron, G., Hirsch, A. I., Worthy, D. E. J., van der Werf, G. R., Randerson, J. T., Wennberg, P. O., Krol, M. C. and Tans, P. P.: An atmospheric perspective on North American carbon dioxide exchange: CarbonTracker, Proc. Natl. Acad. Sci., 104(48), 18925–18930, doi:10.1073/pnas.0708986104, 2007.

Somkuti et al., 2017: Somkuti, P., Boesch, H., Natraj, V., Kopparla, P., Application of a PCA - Based Fast Radiative Transfer Model to XCO2 Retrievals in the Shortwave Infrared, Journal of Geophysical Research: Atmospheres, 122(19), doi: 10.1002/2017JD027013, 2017.

Toon et al., 2009: Toon, G., Blavier, J.-F., Washenfelder, R., Wunch, D., Keppel-Aleks, G., Wennberg, P., Connor, B., Sherlock, V., Griffith, D., Deutscher, N. and Notholt, J.: Total Column Carbon Observing Network (TCCON), p. JMA3, OSA., 2009.

TRD GHG, 2017: Buchwitz, M., Aben, I., Anand, J., Armante, R., Boesch, H., Crevoisier, C., Detmers, R. G., Hasekamp, O. P., Reuter, M., Schneising-Weigel, O., Target Requirement Document, Copernicus Climate Change Service (C3S) project on satellite-derived Essential Climate Variable (ECV) Greenhouse Gases (CO_2 and CH_4) data products (project C3S_312a_Lot6), Version 1, 28-March-2017, pp. 52, 2017.

TRD GAD GHG, 2020: Buchwitz, M., Aben, I., Armante, R., Boesch, H., Crevoisier, C., Hasekamp, O. P., Wu, L.., Reuter, M., Schneising-Weigel, O., Target Requirement and Gap Analysis Document, Copernicus Climate Change Service (C3S) project on satellite-derived Essential Climate Variable (ECV) Greenhouse Gases (CO_2 and CH_4) data products (project C3S_312b_Lot2), Version 2.11, 9-April-2020, pp. 80, 2020.

Wunch et al. 2010: Wunch, D., Toon, G. C., Wennberg, P. O., Wofsy, S. C., Stephens, B. B., Fischer, M. L., Uchino, O., Abshire, J. B., Bernath, P., Biraud, S. C., Blavier, J.-F. L., Boone, C., Bowman, K. P., Browell, E. V., Campos, T., Connor, B. J., Daube, B. C., Deutscher, N. M., Diao, M., Elkins, J. W., Gerbig, C., Gottlieb, E., Griffith, D. W. T., Hurst, D. F., Jiménez, R., Keppel-Aleks, G., Kort, E. A., Macatangay, R., Machida, T., Matsueda, H., Moore, F., Morino, I., Park, S., Robinson, J., Roehl, C. M., Sawa, Y., Sherlock, V., Sweeney, C., Tanaka, T., and Zondlo, M. A.: Calibration of the Total Carbon Column Observing Network using aircraft profile data, Atmospheric Measurement Techniques, 3, 1351–1362, doi:10.5194/amt-3-1351-2010, URL http://www.atmos-meas-tech.net/3/1351/2010/, 2010.

Wunch et al. 2011: Wunch, D., Wennberg, P. O., Toon, G. C., Connor, B. J., Fisher, B., Osterman, G. B., Frankenberg, C., Mandrake, L., O'Dell, C., Ahonen, P., Biraud, S. C., Castano, R., Cressie, N., Crisp, D., Deutscher, N. M., Eldering, A., Fisher, M. L., Griffith, D. W. T., Gunson, M., Heikkinen, P., Keppel-Aleks, G., Kyrö, E., Lindenmaier, R., Macatangay, R., Mendonca, J., Messerschmidt, J., Miller, C. E., Morino, I., Notholt, J., Oyafuso, F. A., Rettinger, M., Robinson, J., Roehl, C. M., Salawitch, R. J., Sherlock, V., Strong, K., Sussmann, R., Tanaka, T., Thompson, D. R., Uchino, O., Warneke, T., and Wofsy, S. C.: A method for evaluating bias in global measurements of CO_2 total columns from space, Atmos. Chem. Phys., 11, 12317-12337, doi: 10.5194/acp-11-12317-2011, 2011.

Copernicus Climate Change Service

ECMWF - Shinfield Park, Reading RG2 9AX, UK

Contact: info@copernicus-climate.eu

climate.copernicus.eu copernicus.eu ecmwf.int